

BLACK MARL EARTHFLOW MOBILITY AND LONG-TERM SEASONAL DYNAMIC IN SOUTHEASTERN FRANCE

J.-P. MALET, O. MAQUAIRE

Institut de Physique du Globe, UMR 7516 CNRS-ULP, 5, rue René Descartes, F-67084 Strasbourg Cedex, France

ABSTRACT: Earthflows in black marl follow a remarkable seasonal kinematic trend induced by the hydrogeological regime and reach high velocities only if significant pore pressure increase takes place. Analysis of the inclinometer observations shows a deformation in a 5-m thick creeping zone with a rigid moving body on top. A first attempt has been made to calibrate three viscoplastic creeping laws on the deformations observed at the Super-Sauze earthflow (Alpes-de-Haute-Provence, France). Calibration was carried out on a period of high pore pressures (and high velocities) and on a period of low pore pressures (and low velocities). Back-analysed cohesion, residual friction angle and viscosity values are quite in accordance with the value measured in the laboratory. Viscosity values are one order of magnitude lower for the high pore pressure calibration period than for the low pore pressure calibration period. Black marls earthflows exhibit a largely non-linear behaviour, with a tendency to plastic behaviour above the critical yield stress. High excess shear stresses induce large deformations and probably a loss of viscous strength leading to infinite acceleration. Therefore, high displacements are predicted for a rise of the ground water level above 1.50 m.

Keywords: Earthflow, Mobility, Black marl, Viscoplastic creep law; Inclinometric observations

1 BACKGROUND

Earthflows are the most typical landslides involving weathered black marl in the Southeastern part of the French Alps. They are generally the result of catastrophic failures in which the initial structural rock block slides transform into a fast moving massive translational landslide progressing downslope, often in natural stream channels. Their movements may result from sliding and flowing, either singly or in combination. Such multiple-mode slope movements exhibit a rapid or slower intermittent movement influenced by slope morphology, rock mass fabric, and hydrology (Hungri et al., 2001).

Earthflows in black marl follow a seasonal kinematic trend induced by the hydrogeological regime and reach high velocities ($>0.05 \text{ m.day}^{-1}$) only if significant pore pressure increases take place, by collapses, stress field changes or unusually infiltration (Malet et al., 2002a). Nevertheless, reworked, predominantly saturated material may continually progress downslope and slowly accumulate in a tongue-like form under normal pore pressure conditions. Continued movement may be maintained over long distances (hectometric to kilometric), depending on the availability of an unobstructed sloping path, and over long periods of time (> 150 years), by intermittent plastic deformation combined with internal creep.

Black marl earthflows are also characterized by their capability to suddenly change behaviour. Under specific hydrogeological conditions, part of the total volume of the moving mass, can transform into debris-flows (Malet et al., 2003).

From a morphological viewpoint, earthflows act as a conveyor belt between the material source and the sink. From a mechanical viewpoint, earthflows exhibit a complex style of movement associating a long-term movement based on creep, and a short-term movement based on flow characteristics. It results in a complex vertical profile of velocity coupling displacements along a shear surface in depth and internal diffuse deformations above this surface. Finally, from an engineering viewpoint, the behaviour of the landslide locates at the interface between soil mechanics (for the long-term movement) and fluid mechanics (for the short-term movement).

While wide areas in mountainous regions are subjected to earthflows movements, especially in soft rocks such as marls or clay shales, a fundamental point to predict their evolution is to develop numerical mechanical models able to reproduce such complex behaviour. Several authors (Vulliet, 1986; Savage and Smith, 1986; Vulliet and Hutter, 1988; Sassa, 1988, Russo, 1997) have suggested that it can be performed by implementing viscoplastic laws in finite-element codes. But it appears that the viscoplastic models have to be calibrated over long time series to really establish the validity of the mechanical assumptions.

This paper focuses on the hydrogeological control of the long-term dynamics of such earthflows, discusses its possible mechanics and calibrates simple viscoplastic creep models to interpret the displacements. The study site is the Super-Sauze earthflow surveyed since 1991, and where extensive geophysical and geotechnical investigations are carried out since 1996.

2 MORPHOLOGY AND BEHAVIOUR OF EARTHFLAWS IN BLACK MARL

2.1 Morphology and internal structure of the earthflows

The Southeastern part of the French Alps consists of sedimentary rocks composed of alternating marl and limestone sequences. In the Barcelonnette Basin, about 100 km north of Nice, three large earthflows (Poche, Super-Sauze and La Valette) have occurred in this formation (Fig. 1a, 1b, 1c). These earthflows are very active and localized in torrential basins (Fig. 1d).

All three landslides are typical earthflows in an intermediate stage of evolution (between stage B and C, -Giusti et al., 1996-) with morphological features clearly recognisable (Fig. 1a, 1b, 1c). The uppermost part of the earthflows is dominated by structural rock block slides at Super-Sauze, rotational slides at La Valette and a combination of both at Poche. Uphill, the main scarp, is inclined at approximately 35° at Poche, 70° at Super-Sauze, and 50° at La Valette. It is cut into morainic deposits (about ten meters thick) and subjacent black marl steep slopes at Poche and Super-Sauze, and into flysch deposits and subjacent black marl at La Valette.

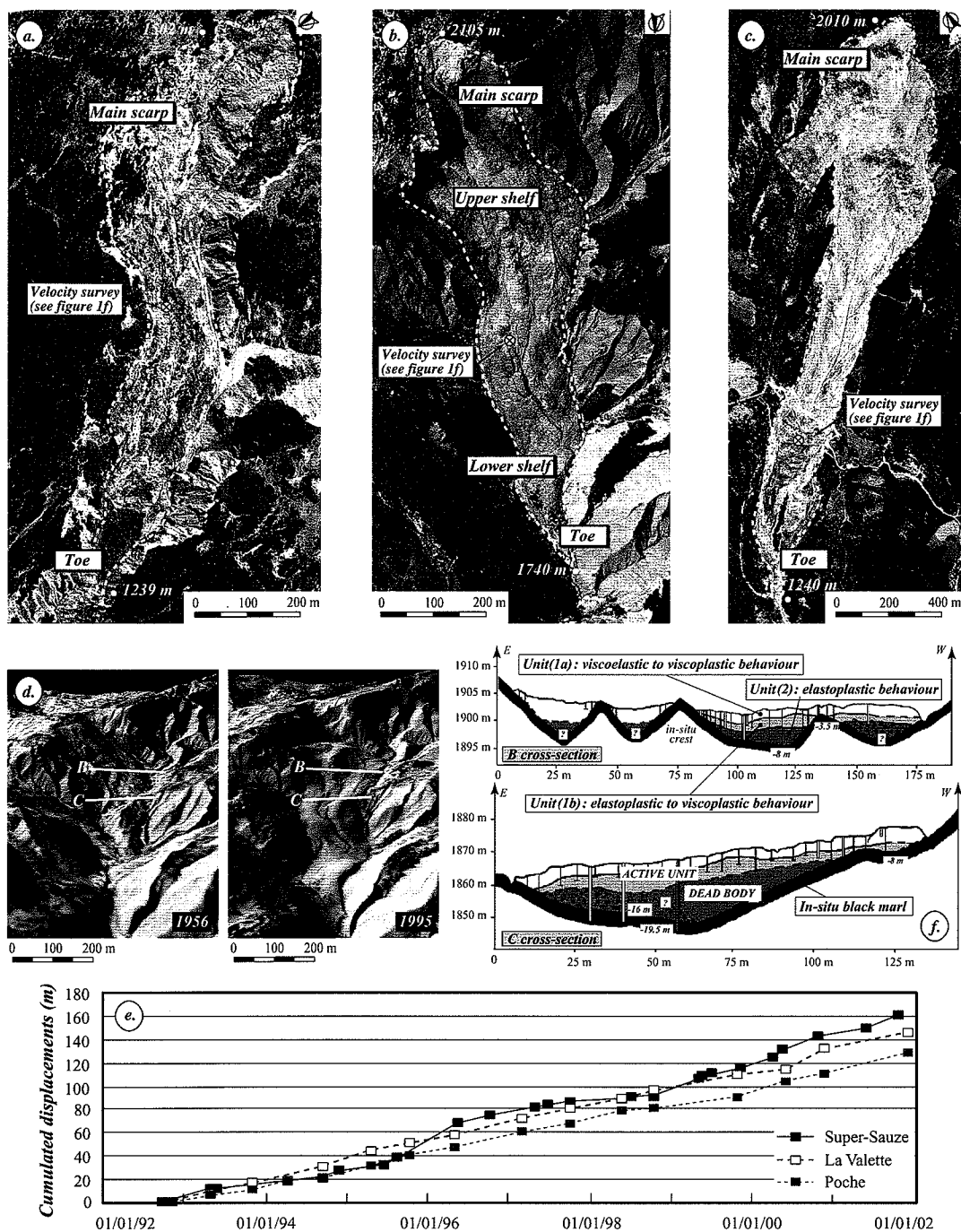


Figure 1. Orthorectified photographs of the Poche (1a), Super-Sauze (1b) and La Valette (1c) earthflows. Reconstitution of the morphological evolution of the Super-Sauze earthflow from 1956 to 1995 (1d). Ten-years cumulated displacements in the central part of the three earthflows (1e). Internal structure of the Super-Sauze earthflow (1f).

Once failed, rock panels are accumulated and progressively disintegrated by weathering. A heterogeneous flow spread out progressively downslope burying torrential channels. The length of the earthflows reaches 1100 m at Poche, 800 m at Super-Sauze, and 1800 m at La Valette. The accumulation zone presents an average slope of 20° for Poche, 25° for Super-Sauze, and 28° for La Valette. Finally, a terminal lobe dominates the lowermost part of the earthflows. Poche and Super-Sauze earthflows are bordered by lateral streams, draining the groundwater tables and adding the contribution of some erosion to the others factors governing the landslide movement. The total volume is estimated at 700,000 to 900,000 m³ for Poche, 750,000 m³ for Super-Sauze and over 3,500,000 m³ for La Valette.

Morphological features induced by the flowing mode of the earthflows are easily recognisable. The contact between the active earthflow and the *in-situ* hillslope is a shearing zone of a

few meters width on both sides of the flow, marked by the presence of tension cracks. Shear surfaces delimiting laterally the earthflows present scratches in the direction of the movement. Locally, lateral levees of compression are distinguishable.

All three earthflows (Fig. 1a, 1b, 1c) exhibit multiple failure mechanisms (within the landslide mass, on the flanks) and involve different material (e.g. black marl rocky panels, black marl weathering products, a silty-sand matrix). Velocities lie in the range from 0.01 to 0.4 m.day⁻¹ for the most active Super-Sauze and La Valette earthflows, and from 0.005 to 0.2 m.day⁻¹ for the less active Poche.

Over the period 1992-2002, the displacements reached 130 m for Poche, 145 m for La Valette, and 160 m for Super-Sauze (Fig. 1e). It is worth noting that the maximal annual displacements are reached for the wettest years of this period, showing the hydro-climatic control of these landslides.

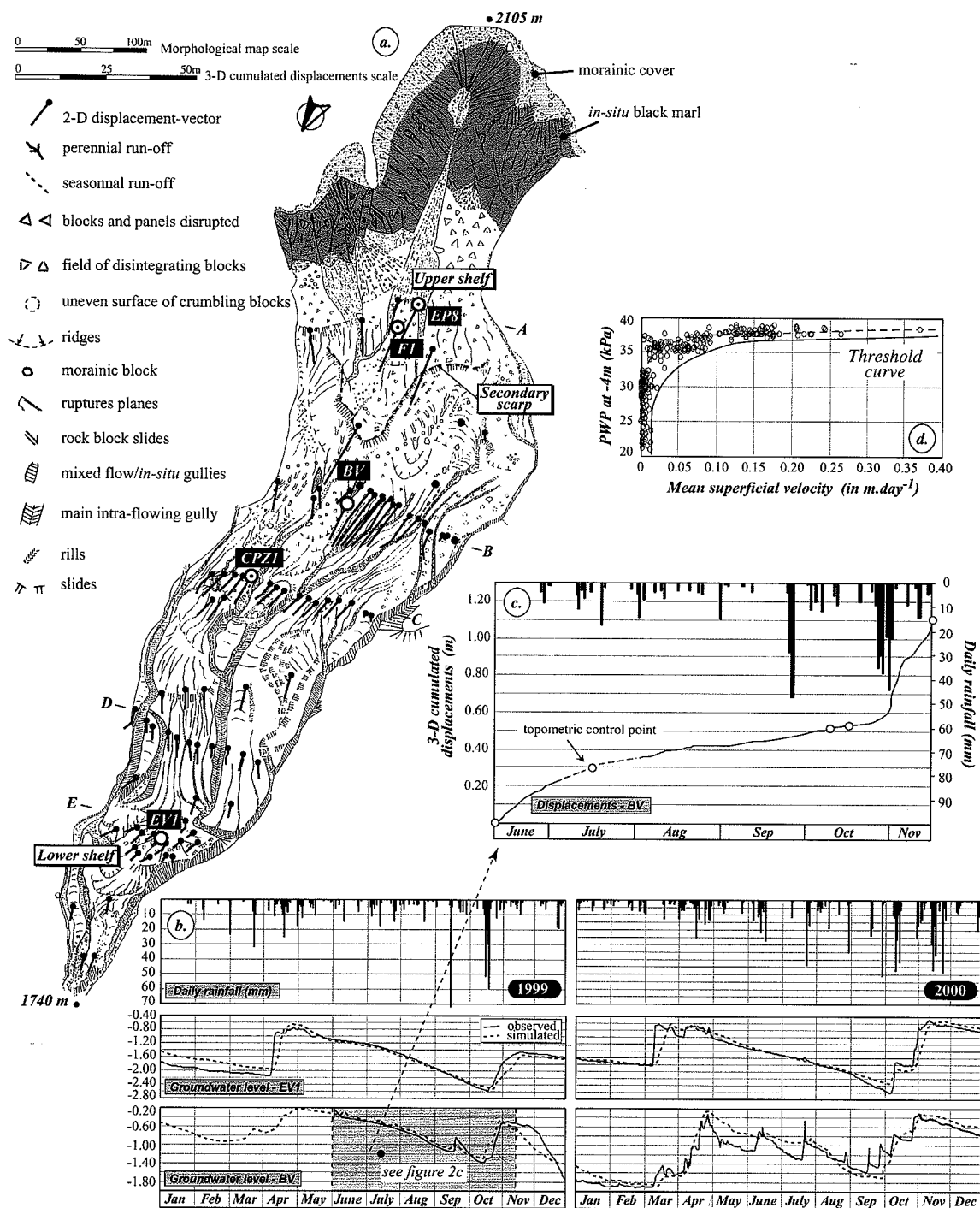


Figure 2. Five-years cumulated displacements of the Super-Sauze earthflow (2a). Observed and simulated groundwater levels over years 1999 and 2000 in the upper and lower part of the Super-Sauze earthflow (2b). Seasonal kinematics of the Super-Sauze earthflow in 1999 (2c). Pore pressure-Velocity relationship (2d).

Geotechnical investigations and geophysical prospecting at Super-Sauze and La Valette (Flageollet et al., 2000; Maquaire et al., 2001) indicate that the flows bury an intact topography formed by a succession of parallel crests and gullies (Fig. 1f). The flow is structured in two vertical units. The first unit (5 to 10 m thick at Super-Sauze and Poche; 10 to 15 m thick at La Valette) is a very wet viscous material, while the second (with a maximum thickness of 10 m, at Poche and Super-Sauze, and 20 m at La Valette) is a stiff and impervious material, referred as a dead body (Le Mignon et Cojean, 2002; Malet et al., 2002a). Both materials involve low plastic intensely fissured reworked marl with a sandy-silt texture (clay content ranging between 16 and 26%; plasticity index ranging between 11 and 19%). Water

content lies between 15 and 40%. For the Super-Sauze earthflow, peak strength parameters, determined on undisturbed samples, show cohesion values ranging from 16 to 37 kPa and friction angle values from 32 to 36°. The residual shear strength was measured by ring shear tests on reconstituted specimens providing a residual friction angle of 19 to 21° (Maquaire et al., in press). This value is in accordance with the operative friction angle calculated with the limit equilibrium method ($\phi'_{mob} = 18^\circ$).

2.2 Long and short-term dynamics of the black marl earthflows

In the following, the data referred to the Super-Sauze earthflow, which is monitored since 1997 (rain gauge, temperature probes,

Casagrande-type piezometers, soil suction probes, extensometric device, GPS monitoring). It is supposed that the behaviour observed at Super-Sauze is representative of Poche and La Valette.

Five years (1997-2001) of continuous displacements and pore water pressures monitoring have demonstrated that its accelerations are totally controlled by hydro-climatic conditions and generally the result of the undrained reactivation of the reworked material; the induced displacements being characterised by a high variable rate. Displacements along the earthflows correspond to the line of greatest slope. The general direction of the displacements is facing N-10° on the cross-sections A, B, C and E and N-340° on the cross-section D and on the toe of the flow, underlining the influence of the paleotopography on the dynamics of the flow (Fig. 2a, 1d). The spatial variability of the displacements along the transverse cross-sections suggest that the landslide body acts as a deformable medium whose behaviour depends on shape of the covered gully (Fig. 1f), on the position of the groundwater table in each compartment, and on the local induced strain field.

All three earthflows are characterized by high groundwater levels. Figure 2b shows an example of the rainfall – groundwater table relationships for years 1999 and 2000 at two locations of the Super-Sauze earthflow. The groundwater level fluctuates from -1.8 m to -0.4 m in the upper part of the flow, and from -2.6 m to -0.8 m in the lower part. The piezometric fluctuations are correlated with rainfall (Malet et al., 2002a). The kinematics follows a seasonal trend with two acceleration periods in spring and in autumn and two deceleration periods (corresponding to hydrological drainage periods) in summer and in winter when snow covers the flow (Fig. 2c). The analysis of the piezometric behaviour shows high pore pressure variations (up to 20-25 kPa corresponding to an average fluctuation of the groundwater level of about 2.5 m) with sudden recharge following the snowmelt. Pore pressures may remain high for a long time due to the low permeability of the reworked marls, and the presence of an impermeable dead body at the bottom. Groundwater table fluctuations follow strictly the same trend all over the earthflow, but the relative position of the water level depends on local conditions. As observed in the field, and as it can be simulated with a hydrological distributed deterministic model (Malet et al., submitted), recharge of the groundwater table is mainly controlled by matrix Darcian flow in the wettest periods of the year (spring) and by a mix of matrix flow and fissure flow the rest of the year.

Two thresholds of pore pressures trigger the acceleration of the movement; above it, the velocity increases non-linearly (Fig. 2d). The “spring movements” are initiated as soon as the water level ranges between -0.8 and -0.7 m below the ground surface; the “autumn movements” are triggered by a higher threshold value (between -0.6 and -0.5 m below the ground surface). This higher level is probably explained by strength regain due to an increase in undrained cohesion by consolidation in summer (Salt, 1988; Van Asch and Bogaard, 1998).

It appears therefore that rainfall is the main triggering factor of the earthflow mobility, producing an intermittent and delayed recharge of the groundwater. The long-term behaviour is characterized by continuous movements with a seasonal trend. The earthflows may be active for decades or more as is justified by the very low Factor of Safety of the landslide body (mean $\phi'_r=20^\circ$, mean slope angle $\beta=25^\circ$) very often below 1. Once a threshold pore pressure distribution is attained, the rate of movement increases. Also, while pore pressures decrease, velocity decreases too, but no stop of the movement is observed. This may be explained considering that both the residual strength parameters and the applied shear stresses are constant with time, as suggested by Picarelli et al. (1999) for clay shale earthflows in the Southern Apennines. Excess pore pressures are therefore only related to infiltration (Malet et al., submitted). This scheme corresponds to the seasonal long-term dynamics of the earthflow. Under exceptional hydroclimatic conditions (conjunction of snowmelt, thawing, and rainfall), short-term dynamics of the earthflow involves the emergence of the groundwater table at the

topographic surface, the evolution of the rheology and the initiation of debris-flows (Malet et al., 2003).

2.3 Vertical profile of velocity

In the ablation zone, the stratigraphic log and the inclinometer observations locate a slip surface at about -8.85 m below the topographic surface for borehole F1 (Fig. 3a) and -8.40 m for borehole EP8 (Fig. 3b). The location of the boreholes on the orthorectified photography of 1956 and 1995 shows that the differences in depth coincide with the location of a gully and a crest (Fig. 3d). Therefore, in the ablation zone, the slip surface presents longitudinally an irregular shape, in relation with those of the initial *in-situ* crests, which were initially 30 to 40 m above (Fig. 2d). In the accumulation zone, the slip surface is located at about -10.50 m (Fig. 3c).

In the ablation zone, the interpretation of the inclinometric profiles and especially the survey of both the displacements of the boreholes and of the depths of shearing (October 1996 to July 2000, cross-section AA', Fig. 3d), indicate both a first slip surface located at -8.85 m, and a second internal slip surface located at around -5.25 m. The first slip surface corresponds to the interface between the dead body and the active unit of the flow.

A careful examination of soil samples taken from the boreholes do not allow to identify a shear “layer” at a depth of approximately -8.85 m. But direct observations on the flanks of a crest emerging from the flow in summer 2001 on the B cross-section, allow detecting such a layer, totally remoulded and saturated, with a thickness of 20 to 30 cm.

From the velocity profile computed for inclinometer F1 (Fig. 3a), it can be supposed that black marl earthflows exhibit a complex style of movement, associating strong displacements along an internal slip surface, located within the reworked landslide body, superimposed by a viscoplastic body (with a shear rate estimated at 10^{-10} m.s⁻¹ assuming a 5-m thick unit) and a rigid body on top (Fig. 3a). Data provided by the other instruments (EP8, CPZ1) validate this point. Similar velocity profiles have also been observed on several landslides (Le Day landslide, Vulliet, 1986; Chlōwena landslide, Vulliet and Bonnard, 1996; Salins-les-Bains landslide, Vans Asch and Boggard, 1998).

Velocity monitoring reveal that stress field change, induced by pore pressure fluctuations, involve the slip surface but also stress the importance of deformability and viscous properties of the landslide body. This implies the use and the implementation of viscoplastic creeping laws in the numerical codes to account for the dependence of the mobilized strength on the displacement rate, such as proposed by Bracerdige et al. (1991), Vulliet (1986), Vulliet and Hutter (1988), Van Asch and Van Genuchten (1991), or Russo (1997).

3 VISCOUS MODELLING OF THE EARTHFLOW

Based on the available data at the location of the inclinometers F1, EP8 and CPZ1, an attempt has been made to apply several viscoplastic creeping laws assuming, in first order, constant pore pressures. All these models assume that above the yield strength the viscous behaviour in the shear zone limits the displacement rate under the excess shear strength., in contrast to the infinite acceleration that is predicted in elastic-plastic models. Here, the viscous behaviour has been described by one empirical relation (Nieuvenhuis, 1991), which relates the viscosity directly to experienced excess in shear stress, and by two physical models (Ter-Stephanian, 1963; Yen, 1969) that incorporate the viscosity as a distinct parameter. The equations and the definitions of the parameters are given in Figure 4 and a review can be found in Van Asch and Bogaard (1998).

For the models, two different definitions of the yield strength and two different definitions of the viscosity parameter η_0 have been tested. In the VCM-1 model (Ter-Stephanian, 1963), the yield strength is defined by a fixed fraction of the peak strength

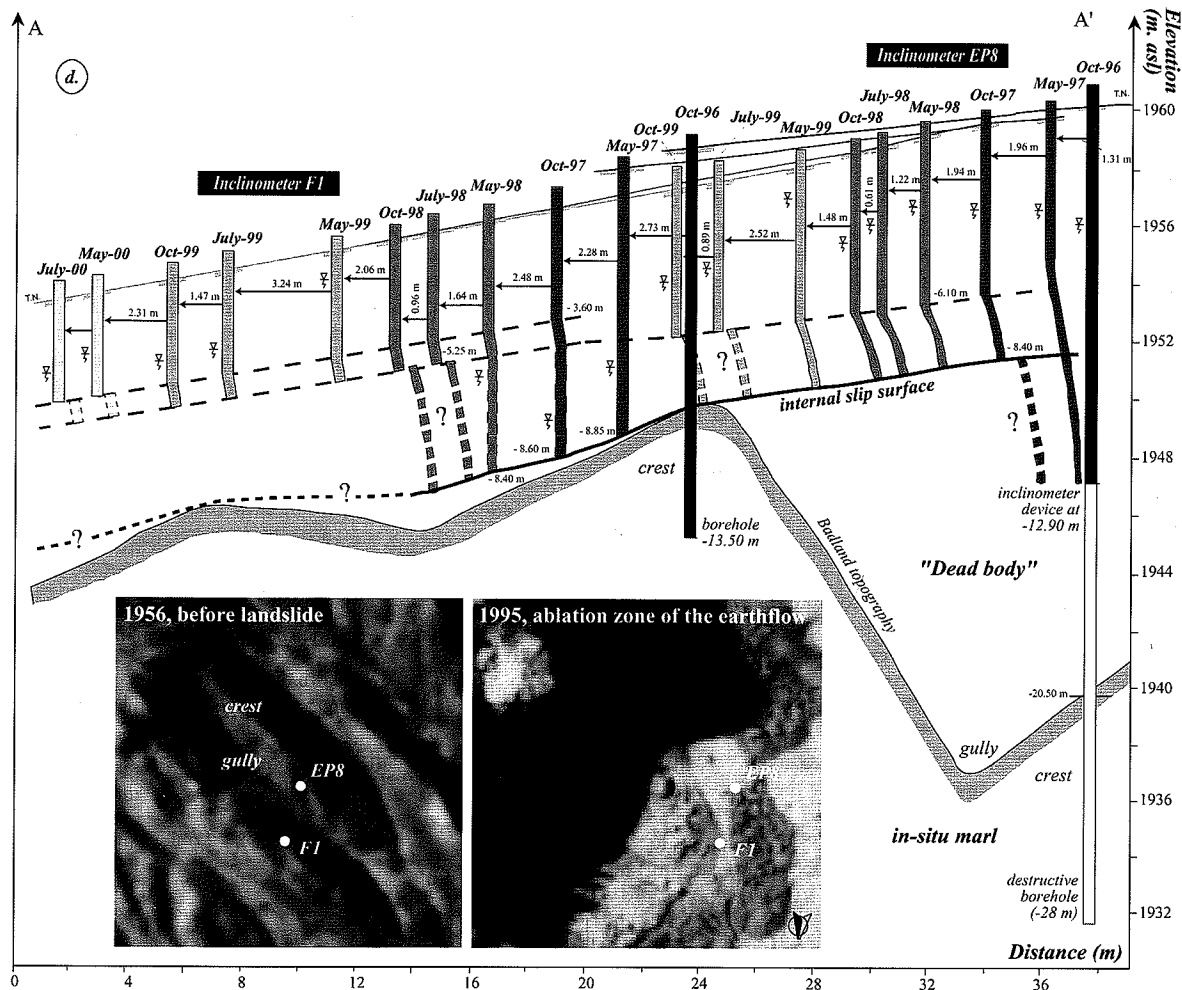
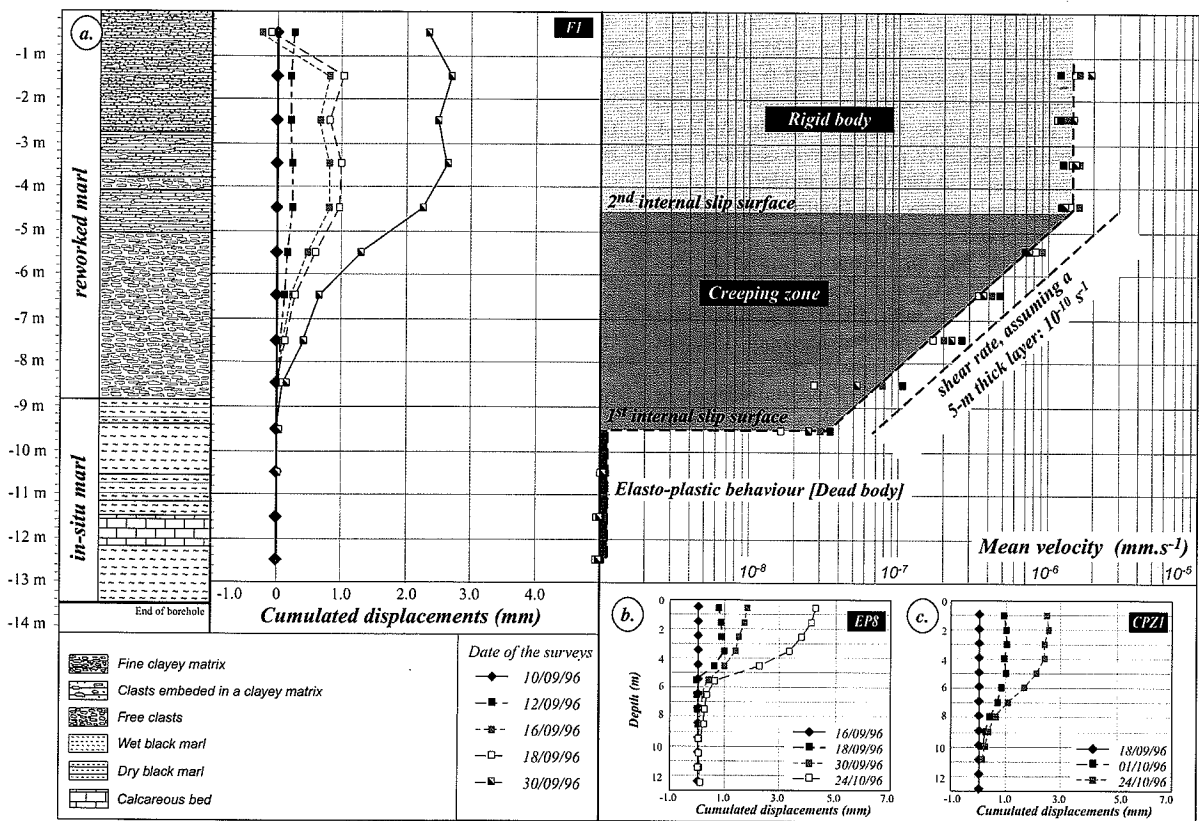


Figure 3. Cumulated in-depth displacements and velocity profile in the ablation zone of the Super-Sauze earthflow (3a, 3b). Cumulated displacements in the accumulation zone (3c). Interpretation of the deformation of the inclinometer tubes in the ablation zone (3d).

values (reduced peak cohesion c'_o , and reduced peak friction angle, ϕ'_o). In the VCM-2 model (Yen, 1969), the yield strength is defined by the residual strength parameters c'_r and ϕ'_r . The viscosity parameter η_o increases with increasing effective normal stress σ , assuming a constant flow factor λ , in the VCM-1 model. On the contrary, the viscosity parameter is constant and independent of the existing stress in the VCM-2 model.

In all cases, the critical yield stress was firstly calibrated for the groundwater levels observed at the onset of the movement, assuming a "spring threshold" and an "autumn threshold" (see section 2.2). Then the viscosity parameter was calibrated given the observed velocities for periods with different groundwater levels. Different scenarios were considered using both different combinations of the yield strength and viscosity definitions, and different deformation profiles (a creep zone of a certain depth, or a deformation limited to the slip surface with a rigid moving body on top).

All models have been calibrated against the derived monthly velocities in $\text{mm}\cdot\text{month}^{-1}$. The choice of this calibration set has been done because velocity is the direct outcome of the models. The goodness of fit is given by the correlation coefficient r^2 , defining the amount of explained variance (Fig. 4a).

4 RESULTS AND DISCUSSION

4.1 Calibration of the creeping laws

In a first step, the empirical Nieuvenhuis' model was tested. The fit of this model is the poorest of all models applied. The predicted displacements are more than half of the observed displacements and the shape of the velocity profile is not well reproduced (Fig. 4b). A possible explanation of the poor fits can be related to the largely non-linear behaviour of the earthflow material, with a tendency to plastic behaviour above the critical yield stress. High excess shear stresses induce large deformations and probably a loss of viscous strength leading to infinite acceleration. This is not well reproduced by the Nieuvenhuis' model. On the contrary, the physical creeping laws have best predictive capacities (Fig. 4a). It is not surprising since both models incorporate in their yield strength definition a significant cohesion value.

In a second step, the influence of the increase in viscosity with depth was evaluated. In this case, two models were considered: the VCM-1a model which comprises the yield strength and viscosity definitions of Ter-Stephanian (1963) and the variant model VCM-1b which comprises the yield strength definition of Ter-Stephanian (1963) and the viscosity definition of Yen (1969). Figure 4b shows the observed and predicted displacement curves for the best-fit simulations. The VCM-1a and VCM-1b curves are similar, indicating that the increase in viscosity with depth has small influences in this case. Both models predict a thinner creeping zone (4 m) than observed in the field (5 m). The back-calculated reduced friction angle ($\phi'_o=14.3^\circ$) seems somewhat too low (Fig. 4a) with respect to the measured peak (36°) and residual (21°) values (Maquaire et al., in press).

Finally, in a third step, the influence of the yield stress definition was evaluated (Fig. 4c). In this case, calibration was carried out using the yield stress definition of Ter-Stephanian (model VCM-1b) and of Yen (model VCM-2), keeping the viscosity constant with depth (Fig. 4c). The VCM-2 model was extensively calibrated, either by optimizing the predicted velocity profile against the observed one (VCM-2a), or the back-calculated residual friction angle against this measured through the laboratory tests (VCM-2b). A calibration was also performed by locating the deformation in a narrow slip surface and assuming an 8.50 m rigid body on top (VCM-2c). The VCM-2a model provides the best fit (Fig. 4a). The model is able to reproduce a 5 m creeping zone, as observed in the field, for a residual friction angle of 26.9° somewhat too high. At the opposite, if the calibration is performed against the residual friction angle (VCM-2b),

the predicted creeping zone is limited to a thickness of 3 m. Finally, the VCM-2c model shows the poorest fit (Fig. 4a).

In all cases, the viscosity values are realistic and consistent with those estimated in the laboratory with a parallel-plate rheometer (Malet et al., 2002b). The viscosity values are lowered by a factor 10 to 100 as the thickness of the creeping zone decreases.

4.2 Prediction of the displacements for different water levels

Considering that the residual strength parameters will govern the reactivation of the earthflow for a specific groundwater level threshold, the viscous properties of the material will govern the amplitude of the movement. Simulations of the displacements have been carried out for different constant (monthly) groundwater levels (ranging from -4 m to -0.5 m), with the higher autumn threshold (Fig. 4d). The best-fit strength and viscosity parameters of model VCM-2 were used. The VCM-2a model shows the best predictive capabilities with a maximal standardized error of 0.23 m. The predicted displacements are extremely limited for mean groundwater levels below -2.5 m., but they can become intolerable for mean groundwater levels higher than -1 m.

The same methodology has been applied for the prediction of displacements initiated by the lower "spring threshold". While no inclinometric observations exist for these periods, an inclinometric profile has been estimated, based on the observed surficial displacements of May 1999 (Fig. 4e). In this case, the results are worse. For instance the VCM-2c model cannot be calibrated (e.g. the model is not able to locate displacements of more than 2 m along a 20 cm-thick shear surface). A creeping zone of 5 m is also not reproduced (VCM-2a, VCM-2b).

For high groundwater levels, the VCM-2a and VCM-2b models are able to predict the cumulated displacements fairly well (Fig. 4e, 4f) by assuming a thickest creep zone and a thicker rigid body. The back-calculated residual friction angle with the VCM-2b model (22°) is consistent with this measured in the laboratory, and a reduction factor (from the peak value to the reduced residual value) of 0.6 can be considered as representative.

In this case, the predicted displacements are extremely limited for mean groundwater levels below -3 m, and become intolerable for mean groundwater levels higher than -1.5 m (Fig. 4f). This feature can be attributed to the viscosity values, lowered by a factor 10 compared to the "autumn threshold". As for the residual strength parameters, it seems that consolidation at periods of lower groundwater levels and no movement, tends to increase viscosity of the material. However, these simulations must be considered as progress results and other viscous laws (Vulliet and Hutter, 1988) should be tested.

4.3 Tentative application to Poche and La Valette earthflows

Despite having any groundwater levels recordings at Poche and La Valette earthflows, a test has been performed with the VCM-2b model to predict the mobility and assess critical conditions.

Table 1. Displacements for different groundwater levels

Groundwater level	Poche earthflow*	La Valette earthflow*
-4.0 m	0 mm / 0 mm	7 mm / 4 mm
-3.0 m	13 mm / 9 mm	32 mm / 19 mm
-2.0 m	38 mm / 27 mm	62 mm / 48 mm
-1.5 m	151 mm / 103 mm	322 mm / 204 mm
-1.0 m	978 mm / 821 mm	1348 mm / 1182 mm
-0.5 m	2150 mm / 1887 mm	2950 mm / 2437 mm

*Spring threshold / Autumn threshold

Simulations have been performed, in the central part of the earthflows, for a one month period, by using the pore pressure thresholds defined at Super-Sauze, and considering: for La Valette, the geometry and structure proposed by Le Mignon and

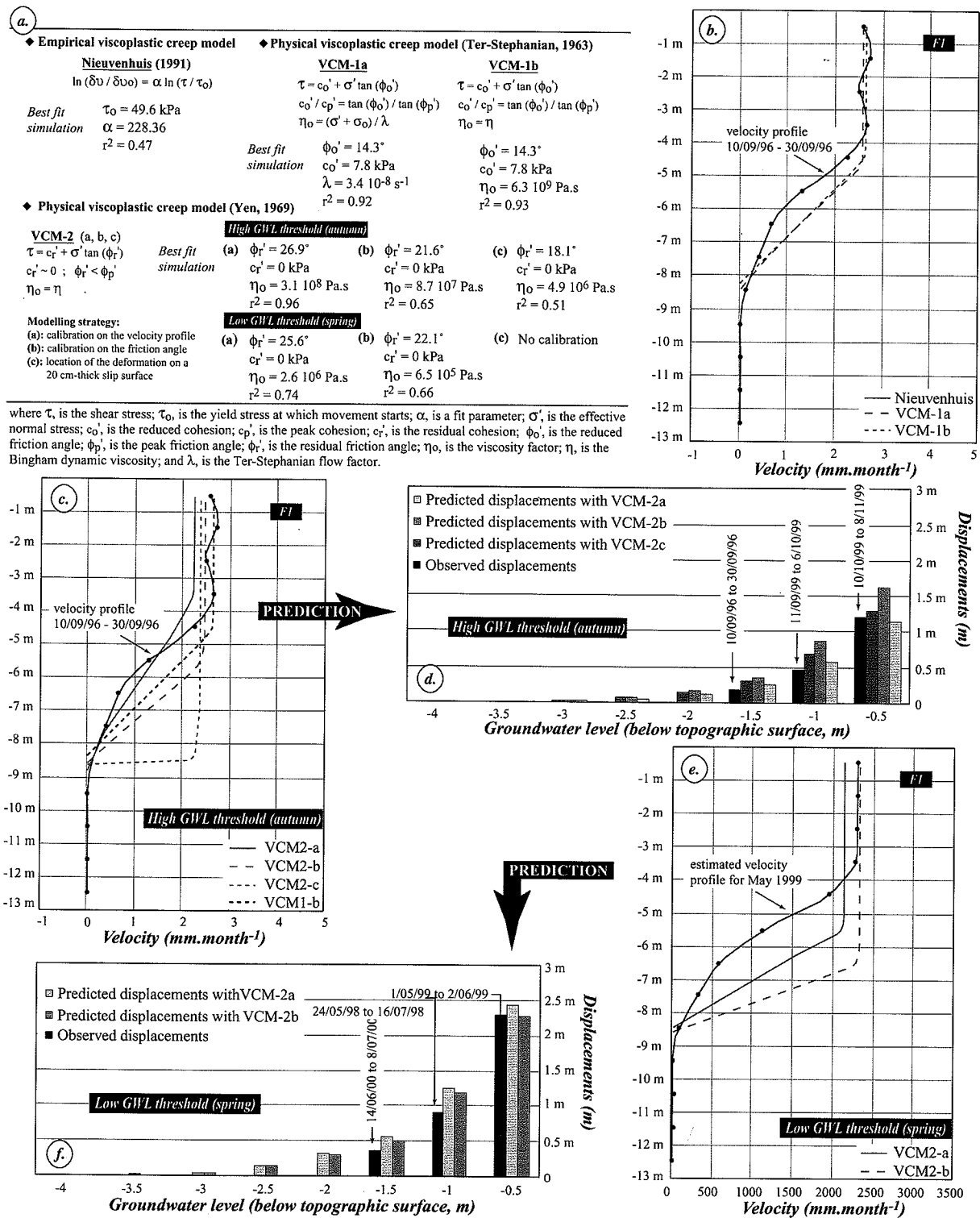


Figure 4. Viscoplastic creep models and applied results of the best-fit simulations (4a). Observed and predicted velocity for a period of low (autumn) groundwater level threshold, according to the Nieuvenhuis and VCM-1 models (4b), to the VCM-2 model (4c) and predicted displacements for different constant ground water levels (4d). Observed and predicted velocity for a period of high (spring) groundwater level threshold, according to the VCM-2 model (4e) and predicted displacements for different constant ground water levels (4f).

Cojean (2001), and the residual strength parameters proposed by Van Beek and Van Asch (1996); and for Poche, the geometry, internal structure and residual strength parameters proposed by Maquaire et al. (in press).

The viscosity parameters obtained through laboratory tests were used for these simulations. Displacements (Table 1) seem acceptable for both earthflows, and intolerable displacements are predicted for groundwater level rise at -1.5 m to -1.0 m below topographic surface.

5 CONCLUSION

Black marl earthflow behaviour is governed by seasonal pore pressure fluctuations inducing long-term movement thanks to the stress changes. First analysis of the inclinometer observations shows a deformation in a creep zone with a rigid moving body on top. Displacements can be interpreted by a simple viscoplastic creeping law assuming constant pore pressures. Calibration was carried out on a period of high pore pressures (and high ve-

locities) and on a period of low pore pressures (and low velocities). Back-analysed residual friction angle and viscosity values are quite in accordance with the value measured in the laboratory. The yield strength is defined by a zero cohesion and a residual friction angle (21°) which is some 60% lower than the peak friction angle. Back-analysed viscosity values are one order of magnitude lower for the high pore pressure calibration period than for the low pore pressure calibration period. There is no evidence that the viscous properties of the flow increase with depth. Both field data and back-analysis reveal that residual strength regain (by consolidation) in the period of drainage of the groundwater table results in two thresholds in pore pressures (spring, autumn) governing acceleration of the earthflows. Decrease in velocity depends both on the duration of the period of pore pressures below these thresholds, and on the viscous properties of the material. Black marls earthflows exhibit a largely non-linear behaviour, with a tendency to plastic behaviour above the critical yield stress. High excess shear stresses induce large deformations and probably a loss of viscous strength leading to infinite acceleration. Predicted surface velocities are in accordance with those measured in the field but the observed deformation profile (a 5-m creep zone overlaid by a 4.50 m rigid body) cannot be recovered. Nevertheless intolerable displacements are predicted for a rise of the ground water level above 1.50 m.

6 ACKNOWLEDGMENTS

This work was granted by the *French Ministry of Research* in the ACI-CatNat contract *MOTE (Modélisation, Transformation, Ecoulement des coulées boueuses dans les marnes)*. We wish to express our gratitude towards the RTM-Barcelonnette, for delivery of measuring results. Contribution INSU N° 336. Contribution EOST N° 2003-032-UMR7516.

7 REFERENCES

- Bracegirdle, A., Vaughan, P.R., Hight, D.W. 1991. *Displacement prediction using rate effects on residual strength*. In Bell, B. (Ed), *Landslides*. Proceedings of the 6th International Symposium on Landslides, 343-347. Rotterdam: Balkema.
- Flageollet, J.-C., Malet, J.-P., Maquaire, O. 2000. The 3-D structure of the Super-Sauze earthflow: a first stage towards modelling its behaviour. *Physics and Chemistry of the Earth*, 25(9): 785-791.
- Giusti, G., Iaccarino, G., Pellegrino, A., Picarelli, L., Russo, C., Urciuoli, G. 1996. *Kinematic features of earthflows in Southern Apennines, Italy*. In Senneset, K. (Ed), *Landslides*. Proceedings of the 7th International Symposium on Landslides, 457-462. Rotterdam: Balkema.
- Hungr, O., Evans, S.G., Bovis, M.J., Hutchinson, J.N. 2001. A review of the classification of landslides of the flow type. *Environmental and Engineering Geoscience*, 7: 221-238.
- Le Mignon, G., Cojean, R. 2002. *Rôle de l'eau dans la mobilisation de glissement-coulées (Barcelonnette, France)*. In Rybar, J., Stemberk, J., Wagner, P. (Eds), *Landslides*. Proceedings of the 1st European Conference on Landslides, 239-244. Lisse: Swets & Zeitlinger.
- Malet, J.-P., Maquaire, O., Calais, E. 2002a. The use of Global Positioning System for the continuous monitoring of landslides. Application to the Super-Sauze earthflow. *Geomorphology*, 43: 33-54.
- Malet, J.-P., Remaître, A., Ancy, C., Locat, J., Meunier, M., Maquaire, O. 2002b. Caractérisation rhéologique des coulées de débris et laves torrentielles du bassin marneux de Barcelonnette. Premiers résultats. *Rhéologie*, 1: 17-25.
- Malet J.-P., Locat, J., Remaître, A., Maquaire, O. 2003. *Dynamics of distal debris-flows induced in clayey earthflows. Implications for hazard assessment*. In Picarelli, L., Sorbino, G. (Eds), *Fast Slope Movements: Prediction and Prevention for Risk Mitigation*. Proceedings of an International Conference. 8p. (this volume).
- Malet, J.-P., van Asch, T.W.J., van Beek, R., Maquaire, O. (in review). Dynamic hydrological modelling of a fast moving complex landslide in the French Alps. *Hydrological Processes*, 18p. (submitted).
- Maquaire, O., Flageollet, J.-C., Malet, J.-P., Schmutz, M., Weber, D., Klotz, S., Guérin, R., Descloîtres, M., Schott, J.-J., Albouy, Y. 2001. Une approche multidisciplinaire pour la connaissance d'un glissement-coulée dans les marnes noires. *Revue Française de Géotechnique*, 95-96: 15-31.
- Maquaire, O., Malet, J.-P., Remaître, A., Locat, J., Klotz, S., Guillon, J. (in press). Instability conditions of marly hillslopes, towards landsliding or gullying? The case of the Barcelonnette Basin, South East France. *Engineering Geology*, 22p. (accepted).
- Nieuwenhuis, J.D. 1991. *Variations in the stability and displacements of a shallow seasonal landslide in varved clays*. Rotterdam: Balkema, 144 p.
- Picarelli, L., Mandolini, A., Russo, C. 1999. *Long-term movements of an earthflow in tectonised clay shales*. In Yagi, N., Yamagani, T., Jiang, J.C. (Eds), *Slope Stability Engineering, Geotechnical and Geoenvironmental Aspects*, 1151-1158. Rotterdam: Balkema.
- Russo, C. 1997. *Caratteri evolutivi dei movimenti traslativi e loro interpretazione meccanica attraverso l'analisi numerica*. PhD Thesis, Università di Napoli, Federico II.
- Sassa, K. 1988. *Geotechnical model for the motion of landslides*. In Bonnard, C (Ed), *Landslides*. Proceedings of the 5th International Symposium on Landslides, 37-55. Rotterdam: Balkema.
- Salt, G. 1988. *Landslide mobility and remedial measures*. In Bonnard, C. (Ed), *Landslides*. Proceedings of the 5th International Symposium on Landslides, 757-770. Rotterdam: Balkema.
- Savage, W.Z., Smith, W.K. 1986. A model for the plastic flow of landslides. *U.S. Geological Survey Professional Paper*, 1385.
- Ter-Stepanian, G. 1963. *On the long-term stability of slopes*. Publication 52, 1-14. Oslo: Norwegian Geotechnical Institute.
- Van Asch, T.W.J., Van Genuchten, P. 1990. A comparison between theoretical and measured creep profiles of landslides. *Geomorphology*, 3: 45-55.
- Van Asch, T.W.J., Bogaard, T. 1998. *A study on the displacements of a landslide near Salins-les-Bains, Eastern France*. In Moore, D., Hungr, O. (Eds), *Proceedings of the 8th International Congress for Engineering Geology and the Environment*, 1641-1646. Rotterdam: Balkema.
- Van Beek, L.P.H., Van Asch T.W. J. 1996. The mobility characteristics of the La Valette landslide. In Senneset, K. (Ed), *Landslides*. Proceedings of the 7th International Symposium on Landslides, 1417-1421. Rotterdam: Balkema.
- Vulliet, L. 1986. *Modélisation des pentes naturelles en mouvement*. PhD Thesis, Ecole Polytechnique Fédérale de Lausanne.
- Vulliet, L., Hutter, K. 1988. Viscous-type sliding laws for landslides. *Canadian Geotechnical Journal*, 25: 467-477.
- Vulliet, L., Bonnard, C. 1996. *The Chlövrena landslide: prediction with a viscous model*. In Senneset, K. (Ed), *Landslides*. Proceedings of the 7th International Symposium on Landslides, 397-402. Rotterdam: Balkema.
- Yen, B.C. 1969. Stability of slopes undergoing creep deformation. *Journal of the Soil Mechanics and Foundation Engineering Division*, SM 4: 1075-1096.